

We are IntechOpen, the world's leading publisher of Open Access books Built by scientists, for scientists

4,800

Open access books available

122,000

International authors and editors

135M

Downloads

Our authors are among the

154

Countries delivered to

TOP 1%

most cited scientists

12.2%

Contributors from top 500 universities



WEB OF SCIENCE™

Selection of our books indexed in the Book Citation Index
in Web of Science™ Core Collection (BKCI)

Interested in publishing with us?
Contact book.department@intechopen.com

Numbers displayed above are based on latest data collected.
For more information visit www.intechopen.com



The Influence of Proteins Surface on the Ordering of Surrounded Water

Mateusz Banach, Leszek Konieczny and Irena Roterman

Additional information is available at the end of the chapter

Abstract

Protein folding remains not satisfactory understood process. Considering the critical importance of water for proteins and other biologically active molecules, analysis of water-protein interactions should play a central role in studies concerning the folding process and biological activity of proteins. Folding simulations should acknowledge the aqueous solvent as an active partner which determines the final conformation of a protein. In the fuzzy oil drop model (which is applied in the presented analysis), the solvent is treated as a continuum—an external force field guiding the folding process. This interaction goes both ways: (1) the solvent shapes the protein and (2) the presence of a natively folded protein also alters the structure of the solvent (the structure of water has not heretofore been sufficiently studied—except for the solid state). This work focuses on this second reverse relationship, that is, the influence of proteins upon the structuralization of water. We formulate a hypothesis which is based on the fuzzy oil drop model. The ordering of the hydrophobic core which resides inside the protein and may include local discordances is analyzed from the point of view of its external effects. In accordance to the fuzzy oil drop model, the solvent is expected to “react” to local differentiation in the properties of the molecular surface. Our hypothesis remains speculative, since experimental studies have not yet yielded sufficient evidence to either prove or disprove it. The presented analysis bases on the assumption that a protein is nothing more than a tool engineered to perform a specific task. Thus, the protein’s structure must encode its intended use and the inter-molecular communication system. Our study focuses on antifreeze proteins, which are particularly interesting since their function involves altering the properties of the solvent—specifically, preventing the formation of ice crystals.

Keywords: hydrophobicity, protein structure, hydrophobic core, water-protein surface interface, role of exposed hydrophobicity on protein surface

1. Introduction

Protein folding continues to attract a great deal of scientific interest in hopes of discovering its underlying mechanisms [1–6]. The search for computational algorithms is capable of reliably predicting the conformational properties of specific residue chain dates back to at least 1994, which is when the CASP challenge was launched [7]. That each residue sequence encodes a specific 3D structure is evident from the fact that protein folding—which continually occurs in living organisms—produces the same results each time [8, 9]. To-date protein folding models fail to acknowledge the involvement of the aqueous solvent, which plays a crucial role not only in protein folding, but also in other processes occurring in living cells. In molecular dynamics simulations, water is typically modeled as a set of molecules (expressing the known solvent density) [8, 10]. These molecules interact with polypeptide chain atoms in a pairwise (atom-atom) fashion.

In contrast, the fuzzy oil drop model which underpins the presented research treats the solvent as a continuum whose structural properties are unknown (for example, it is unclear why the density of water peaks at 4°C) but whose effects can be observed experimentally. The polar solvent causes hydrophobic residues to congregate at the center of the protein body, while hydrophilic residues are instead exposed on its surface. Nevertheless, hydrophobic residues are not perfectly isolated and can be detected on the surface of many proteins.

Rather than delve into the structural properties of proteins, the presented analysis focuses on the reverse relationship—the effect of the protein’s presence upon the surrounding environment. This issue is important in light of the variable degree of ordering (or disorder) which characterizes the protein’s hydrophobic core. More specifically, it refers to the occasional exposure of hydrophobicity on the surface and—by the same token—internalization of hydrophilic residues. Clearly, regardless of the structure of the solvent (which is treated as a continuum), exposure of hydrophobicity must result in local changes in its properties.

The assumption which forms the basis of the presented work is that the 3D structure of a protein represents a balance between the effects of internal force fields (pairwise interactions between atoms) and the external force field (the aqueous solvent, treated as a continuum).

In order to provide a mathematical model of the solvent, we refer to a 3D Gaussian form, which is assumed to represent an idealized (or “theoretical”) distribution of hydrophobicity in a perfect protein molecule—with all hydrophobic residues internalized and all hydrophilic residues exposed on the surface. It turns out that while actual proteins do indeed conform to this model, they also exhibit certain deviations and localized discordances, which are associated with their function. For example, local exposure of hydrophobicity usually forms a suitable interface for protein-protein interactions [11–14], while local hydrophobicity deficiencies often characterize ligand/substrate binding cavities [15]. In addition to such localized effects (which can be formally quantified), the protein as a whole may diverge from the theoretical model by adopting an entirely different structural pattern, precluding the formation of a hydrophobic core. Such effects are observed, for example, in solenoid fragments, where

instead of a centralized core we are faced with linear propagation of alternating bands of high and low hydrophobicity. This group also includes antifreeze proteins and pathological structures referred to as amyloids [16]. The difference between both groups is that antifreeze proteins contain—in addition to solenoid fragments—additional structural units which are locally accordant with the 3D Gaussian and provide the protein with solubility. Amyloids lack such structures and therefore remain insoluble [17, 18].

The presence of a protein in which the distribution of hydrophobicity is not in perfect agreement with environmental stimuli must exert an influence upon the environment itself. Exposure of hydrophobicity is “felt” by adjacent water molecules, which then react accordingly. This reverse relationship between a fully folded protein and the aqueous solvent is the focus of the presented study.

One of the major concepts in physical chemistry is the phenomenon of micellarization, producing various types of micelles (including spherical micelles) [16]. Bipolar molecules which comprise both hydrophobic and hydrophilic components aggregate to form structures which limit the entropically disadvantageous contact between hydrophobic fragments and water in favor of exposure of polar fragments [19–22].

The surfactant micelle, made up of identical loose units, exhibits high symmetry. This symmetry is additionally promoted by the large number of degrees of freedom characterizing each unit molecule—much like in the case of spherical or wormlike micelles [19–22].

The micelle may also intercalate external molecules, regardless of their size, if these molecules are capable of aligning themselves with the solvent without disrupting the overall symmetry of the system [23–25]. In all such cases, the surface of the micelle must be uniformly composed of polar groups, ensuring entropically advantageous interaction with water.

Of course, treating the protein as a “quasi” micelle, with properties similar to those exhibited by surfactant micelles, comes with certain caveats. The principal differences between proteins and surfactant micelles are twofold: first, in a residue chain, the distribution of hydrophobicity varies from amino acid to amino acid; second, the residues forming a polypeptide are not individual molecules—rather, they are connected with peptide bonds which significantly restrict their conformational freedom and therefore their ability to reach a location which would reflect their intrinsic hydrophobicity. Consequently, proteins do not follow the idealized distribution with perfect accuracy. Although it is, in principle, possible to design a sequence which would fold into a near-perfect spherical micelle, with excellent agreement between the theoretical and observed distribution of hydrophobicity [26], the vast diversity of biologically active proteins suggests that some proteins may be unable to generate a prominent central hydrophobic core. This, in turn, implies that the type and degree of local/global discordance versus the theoretical model are an expression of the quality referred to in biochemistry as “specificity”. It should, however, be noted that in our study, the term does not refer to specificity of chemical interactions (e.g., between the protein and its ligand) but rather to the specific relation between the protein and the aqueous solvent, which is intimately linked to the existence and activity of numerous proteins.

The structural properties of water remain poorly understood—as evidenced by the lack of a convincing explanation of why the density of water peaks at 4°C. For this reason, we postulate extension of further experimental analysis of the aqueous solvent as a critical factor in mediating communication between molecules forming the solute. Further insight in this regard would help explain how the presence of water affects the protein—but also how the presence of proteins affects the solvent. The water environment shall also be treated as medium for inter-molecular communication. The characteristics of protein surface seem to play a critical role in this issue. This is why we attempt to demonstrate that the relationship water-protein is mutualistic.

2. Materials and methods

2.1. Data

The presented analysis concerns antifreeze proteins listed in **Table 1** (along with brief descriptions).

The study set presented in **Table 1** was assembled in an intentional manner. The protein—1J5B (type I antifreeze protein)—is a simple helix with highly discordant, however, very specific hydrophobic core. 2ZIB (type II antifreeze protein) exhibits minor discordance versus the model. The set is complemented by a globally discordant protein—multidomain antifreeze protein (5B5H) and a pathological (amyloid-2MVX) protein in which the distribution of hydrophobicity is entirely linear and consists of alternating bands of high and low hydrophobicity.

The discordances exhibited in each protein are quantified by applying methods described in the following subsection.

2.2. Fuzzy oil drop model

The fuzzy oil drop model has been thoroughly described in numerous publications with detailed presentation [31]. The authors also presented its application to antifreeze proteins [16] as well as to pathological proteins (amyloids) [17, 18]. For the purposes of the presented research, we will limit ourselves to a brief recapitulation of the model's core concepts, enabling the reader to understand the results presented further below.

PDB-ID	Protein	Chain length	Reference
Helix-1J5B	Antifreeze I type	37 aa	[27]
Globular-2ZIB	Antifreeze II type	130 aa	[28]
Solenoid-5B5H	Antifreeze-multidomain	223 aa	[29]
Amyloid-2MVX	Amyloid	73 aa/chain	[30]

Table 1. Set of proteins subjected to analysis, along with their basic properties and selected references.

At its heart, the fuzzy oil drop model is a modification of Kauzmann's original oil drop model [32]. That model likens the folding polypeptide to a drop of oil which—being a hydrophobic substance—attempts to limit the area of its contact with the aqueous solvent. Kauzmann divides the 3D protein structure into two layers: the internal (hydrophobic) layer and the external (polar) layer. The fuzzy oil drop model replaces this binary division with a continuous distribution where hydrophobicity peaks at the center and then progressively decreases along with the distance of the center, reaching almost 0 on the protein surface. This distribution can be mathematically expressed as a 3D Gaussian. If the protein molecule is encapsulated in a virtual ellipsoid (whose dimensions are adjusted to match the actual size of the protein), the Gaussian function directly yields the theoretical hydrophobicity values for arbitrary points within this capsule.

In mathematical terms, the 3D Gaussian is defined as follows:

$$\tilde{H}t_j = \frac{1}{\tilde{H}t_{sum}} \exp\left(\frac{-(x_j - \bar{x})^2}{2\sigma_x^2}\right) \exp\left(\frac{-(y_j - \bar{y})^2}{2\sigma_y^2}\right) \exp\left(\frac{-(z_j - \bar{z})^2}{2\sigma_z^2}\right) \quad (1)$$

$\bar{x}, \bar{y}, \bar{z}$ reflect the placement of the center of the ellipsoid (all three are equal to 0 at the origin of the coordinate system). σ coefficients are calculated as 1/3 of the greatest distance between any effective atom belonging the molecule and the origin of the system, once the molecule has been oriented in such a way that its greatest spatial extension coincides with a specific axis (for each axis separately).

The $1/\tilde{H}t_{sum}$ coefficient ensures the normalization of both distributions (empirical and theoretical) and therefore enables comparative analysis. While theoretical hydrophobicity is defined at any point within the encapsulating ellipsoid, in practice, we are only interested in positions that correspond to effective atoms (averaged-out positions of all atoms comprising a given residue). Consequently, the sum has N components, where N is the number of residues in the chain. Each component is the theoretical value of hydrophobicity at the position of the given.

In contrast to the above, the actual distribution of hydrophobicity may diverge from theoretical values. Observed hydrophobicity (O) results from interactions between adjacent amino acids, which, in turn, depend on their mutual separation and the intrinsic hydrophobicity of each residue (which can be determined experimentally or on theoretical grounds [33]). Our analysis is based on the intrinsic hydrophobicity scale proposed in [31]. Under these assumptions, the observed hydrophobicity is given by the following formula [34]:

$$\tilde{H}o_j = \frac{1}{\tilde{H}o_{sum}} \sum_{i=1}^N (H_i^r + H_j^r) \begin{cases} \left[1 - \frac{1}{2} \left(7 \left(\frac{r_{ij}}{c} \right)^2 - 9 \left(\frac{r_{ij}}{c} \right)^4 + 5 \left(\frac{r_{ij}}{c} \right)^6 - \left(\frac{r_{ij}}{c} \right)^8 \right) \right] & \text{for } r_{ij} \leq c \\ 0 & \text{for } r_{ij} > c \end{cases} \quad (2)$$

In both equations (Eqs. (1) and (2)), j denotes the position of the effective atom of the j -th residue. Ho_j is an aggregate value describing the interactions with neighboring residues (indexed i) at a distance not greater than 9 Å (this distance, c , is treated as the cutoff value

for hydrophobic interactions, following the original model [34]). Applying a cutoff value implies that hydrophobic interactions are considered local and depend on the position of each residue. This function is empirically determined and, according to [34], expresses the force of hydrophobic interactions. H_i^r and H_j^r represent intrinsic hydrophobicity (constant for each residue) according to a predetermined scale, which can be arbitrary (in our study, the relevant scale is derived from [31]). r_{ij} is the distance between the i -th and the j -th residue, while N is the total number of residues in the chain.

Normalization of both distributions (with all T_i and all O_i adding up to 1.0) facilitates quantitative comparisons, as illustrated in **Figure 1**. Differences between both distributions may vary. **Figure 1A** shows a protein where the observed distribution is closely aligned with the theoretical distribution, while **Figure 1B** illustrates the opposite case—a significantly discordant protein.

Subjective assessment of the degree of discordance (cf. **Figure 1**) may be supplemented by quantitative analysis based on Kullback-Leibler's divergence entropy formula [35]:

$$D_{KL}(p|p^0) = \sum_{i=1}^N p_i \log_2(p_i/p_i^0) \quad (3)$$

where D_{KL} represents the distance between two distributions: "observed" (p) and "target" (p_0).

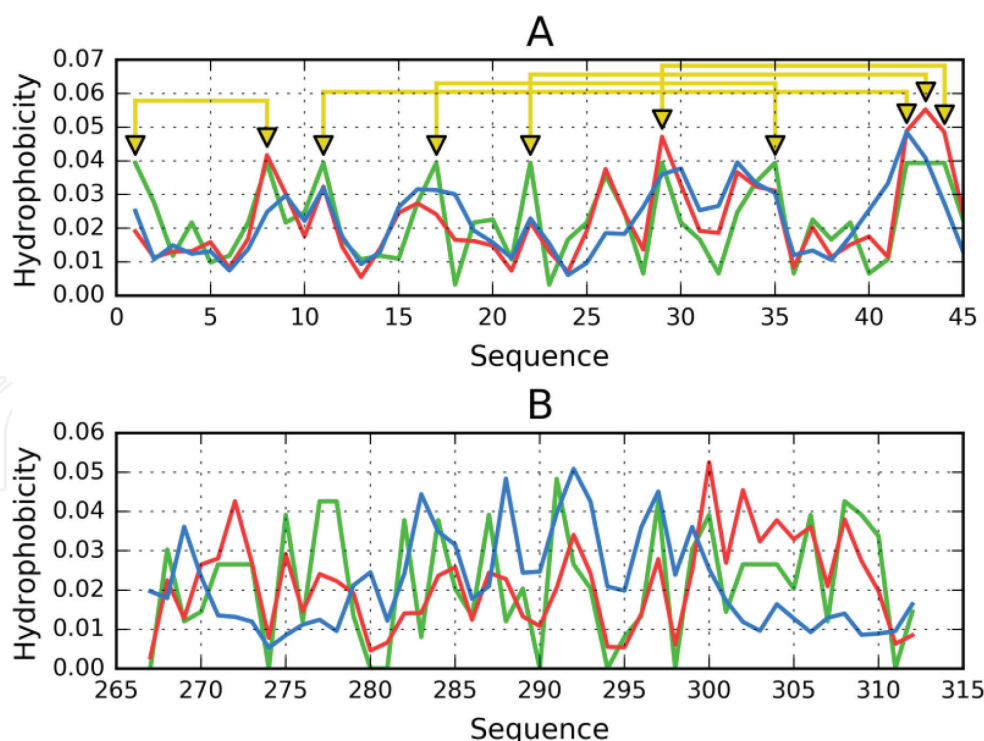


Figure 1. Examples of two proteins that differ with regard to their hydrophobic core structure: (A) accordant protein (5LAH-45 aa [35]) and (B) discordant protein (2MZ7-46 aa [36]). These proteins were selected to illustrate strong conformance/strong discordance, and are not part of the study set analyzed in this chapter. The disulphide bonds are shown as yellow lines.

To provide a quantitative measure of the differences between O and T, the latter distribution will be treated as a reference.

The status of a given protein is represented by D_{KL} values, which express its proximity to reference distributions treating distribution T as p^0 and distribution O as p :

$$O|T = \sum_{i=1}^N O_i \log_2(O_i/T_i) \quad (4)$$

The opposite reference distribution, R, represents the distribution deprived of any form of hydrophobicity differentiation (each residue represents equal hydrophobicity $R_i = 1/N$, where N is the number of residues in protein). The corresponding O | R relation is defined as follows:

$$O|R = \sum_{i=1}^N O_i \log_2(O_i/R_i) \quad (5)$$

For the examples illustrated in **Figure 1**, D_{KL} for protein (A) is 0.08, while for protein (B), its value is equal to 0.46.

These values cannot, however, be considered on their own, since D_{KL} is a relative measure of relative entropy (and moreover depends strongly on the number of residues in the chain). Introduction of two reference distributions allows the comparison: O | T larger than O | R suggests similarity between O and R distribution.

In order to avoid having to deal with two distinct values, we further introduce the so-called relative distance parameter, defined as follows:

$$RD = O|T / (O|T + O|R). \quad (6)$$

Values lower than 0.5 mean that O is a better match for T than for R. This is interpreted as the presence of a centralized hydrophobic core.

For the examples illustrated in **Figure 1**, RD values are 0.300 (A) and 0.680 (B), respectively.

It should be noted that various distributions may be used as reference. Besides R, we may also introduce another distribution, denoted H, which corresponds to the intrinsic hydrophobicity of each residue. In this case, the value of RD will express whether the given protein exhibits a distribution which more closely resembles T or H. Accordingly, we obtain two distinct values of RD: one for the T-O-R model and one for the T-O-H model. Such analysis becomes helpful when studying amyloid structures, which, according to FOD-based analysis, appear to be dominated by the conformational preferences of individual amino acids with no regard for the creation of a global hydrophobic core (unlike in globular proteins) [36]. To further underscore the influence of intrinsic hydrophobicity, we may also calculate correlation coefficients for three types of relationships: HvT, TvO, and HvO. We will soon show that strong discordance between O and T, where no centralized hydrophobic core can be observed, leads to negative HvT and TvO correlation coefficients, along with high positive values of the HvO coefficient.

2.3. The aqueous solvent—an interpretation rooted in the fuzzy oil drop model

Protein folding is regarded as the search for a global energy minimum. This implies optimization of the protein's internal force field. Nonbinding interactions (electrostatic, vdW, torsional potential, and others) are present in every molecule and produce structural forms which are optimal from the point of view of free energy minimization.

Classic protein folding algorithms (mostly based on molecular dynamics simulations) acknowledge the presence of the solvent by including a set number of external water molecules that interact with atoms belonging to the protein chain [12]. In contrast, the fuzzy oil drop model treats water as a continuum, represented by an external force field which directs hydrophobic residues toward the center of the molecule while exposing polar residues. This effect—next to the formation of disulfide bonds—is regarded as a primary force which stabilizes the protein's tertiary conformation.

The presented model therefore acknowledges the role of the solvent with no in-depth knowledge regarding the properties of this solvent: its mere presence is enough to drive the folding process, producing structures which are largely consistent with the 3D Gaussian distribution of hydrophobicity [26].

In fact, the structural ordering present in proteins is highly varied and may include local or global discordances. A local discordance manifests itself as either local excess hydrophobicity on the protein surface (providing a complexation interface for p-p interactions [11, 12]) or local deficient hydrophobicity inside the protein body (which often characterizes ligand or substrate binding pockets [13, 14]). On the other hand, global discordance occurs when the entire protein follows a different structural pattern which does not involve a centralized hydrophobic core—for example, linear propagation of alternating bands of high and low hydrophobicity, as observed in amyloid [17, 18].

Analysis of the observed distribution of hydrophobicity tells us whether the protein conforms to the theoretical model (and if it does—whether it includes any local deviations) or diverges from the model entirely.

The presented work focuses on the reverse phenomenon, that is, the influence of the protein upon its environment. Naturally, this is merely a postulate based on the observed nonalignment between O and T for many biologically active proteins. In such cases, the protein itself may be treated as the source of an external force field which acts upon the solvent. Its presence alone is sufficient to direct nearby water molecules. This phenomenon may potentially serve as a carrier of information between proximate proteins—a notion upon which the so-called iceberg hypothesis is based [37, 38].

One example which provides strong support for the above thesis involves antifreeze proteins. Such proteins are expected to work by disrupting the natural structuralization of water and thereby preventing formation of ice crystals. The explanation provided by our model contradicts older analyses, which search for ways in which nascent ice crystals might potentially dock to antifreeze proteins [39]. In our view, no such docking takes place. The docking model is also overly sensitive to concentrations of antifreeze proteins and does not explain

the antifreeze effect observed in the context of small particles, for example, saccharides [39] or phospholipids [40]—not to mention individual ions, which are also observed to prevent formation of ice crystals in the macro scale.

3. Results

The effect of the presence of proteins upon the aqueous solvent is particularly evident in the case of antifreeze proteins [41]. Their task is to keep water from freezing in subzero temperatures, which would otherwise destroy cells and tissues, terminating all processes which the organism relies on in order to function. The increased mobility of water molecules on the surface of antifreeze proteins observed experimentally supports this expectations [42].

Organisms which undergo hibernation (including fish, plants, and other organisms) [41] have been found to produce specific proteins whose role is to counteract the formation of ordered ice crystals. Referring to calcium and sodium ions, if we assume that their presence disrupts the coordination of water particles (an effect exploited, e.g., for salting roads during winter), the same should be expected in the case of the aforementioned proteins.

The presented proteins have been intentionally selected in order to highlight various ways in which proteins affect the local structure of the aqueous solvent and counteract its tendency to crystallize.

3.1. Small (type I) antifreeze proteins

Type I antifreeze proteins are small and exhibit a uniform secondary structure, that is, they are entirely helical. One example is 1J5B, as listed in **Table 2**. **Figure 2** presents the theoretical and observed hydrophobicity distributions for this protein.

As evident in **Figure 2**, in place of the expected central hydrophobicity peak, we are faced with a near-sinusoidal pattern. Notably, the cyclical nature of this distribution does not correspond to individual twists which comprise the alpha helix (the number of residues per distribution cycle appears greater than 3). If this were the case, we would be dealing with a perfectly amphipathic helix, whereas the observed periodicity of changes results

Protein	RD		Correlation coeff.		
	T-O-R	T-O-H	HvT	TvO	HvO
1J5B	0.767	0.557	0.221	0.450	0.860
2ZIB	0.556	0.392	0.201	0.531	0.687
2ZIB No 70-78	0.498	0.361	0.214	0.572	0.693

Removal of the 70-78 fragment in 2ZIB produces a chain which is accordant with the theoretical distribution of hydrophobicity (position No 70-78).

Table 2. Small antifreeze proteins—fuzzy oil drop parameters.

in strong variations in the structural properties of water in close proximity of the protein. Hydrophilic patches likely attract water molecules resulting in an energetically optimal arrangement; however, in hydrophobic areas, the structuralization of water, while not precisely known, is most likely significantly altered (whatever the word “altered” means in this context). Water has been found to exhibit increased mobility close to antifreeze proteins, likely as a result of its complex interactions with the molecular surface [42]. It is postulated that the protein causes vortices to form in the surrounding medium (as illustrated in **Figure 3**).

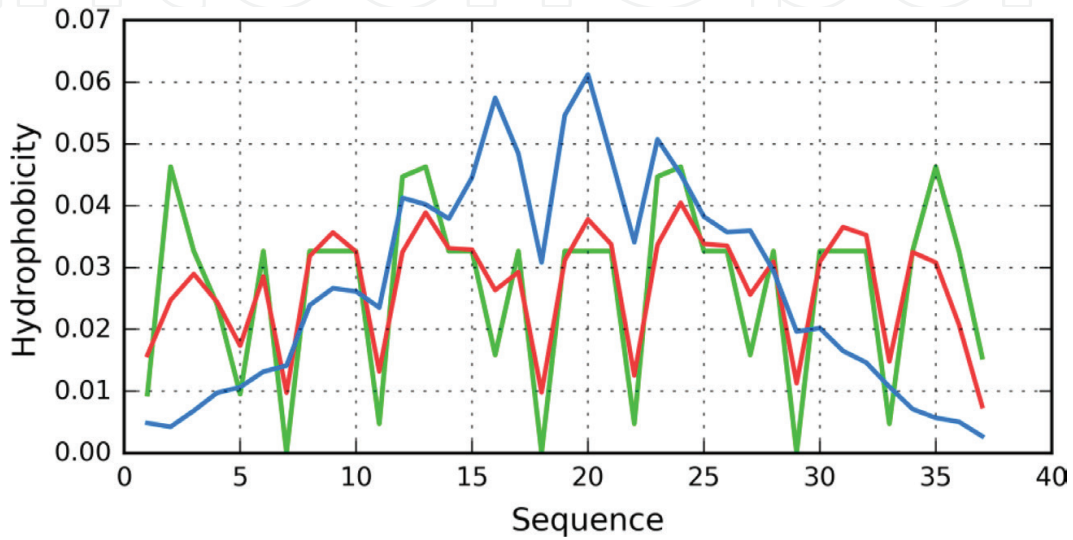


Figure 2. Type I antifreeze protein (IJ5B)—the figure illustrates the misalignments between T (blue) and O (red). The H distribution—green line.



Figure 3. The distribution of hydrophobic residues along the helix does not correspond to its structural periodicity. The image schematically depicts the expected reaction of the surrounding water particles, which are either attracted (teal) or repelled (red) by the molecular surface.

3.2. Small protein exhibiting marginal local discordance—2ZIB

2ZIB, with a chain length of 130 aa, provides an example of a type II antifreeze protein. Taken as a whole, it is characterized by RD slightly in excess of 0.5 (**Table 2** and **Figure 4**). Similar RD values in the T-O-R and T-O-H models, as well as comparable correlation coefficients, suggest that all factors (T, H, and O) represent some sort of consensus.

Figure 5 reveals the location of hydrophobic residues close to the surface. While most of the surface is composed of hydrophilic (polar) residues, local exposure of hydrophobicity produces a change in the structural properties of water as individual dipoles align themselves with the protein. The resulting structure disfavors ice crystal formation.

Removing the fragment at 70-78 (**Table 2**) produces a chain which largely conforms with theoretical expectations (95% of the remaining structure is accordant with the theoretical model). As noted, the presence of a charged surface induces changes in the structuralization of the aqueous solvent and thereby counteracts ice crystallization. It appears that the protein performs its function in much the same way as Na^+/Cl^- ions—with the added benefit of being able to expose a much larger surface area and thereby exert a more significant effect upon the surrounding medium.

The protein under consideration is also characterized by unexpectedly large number of disulfide bonds—in the chain of 130 aa, there are 5 SS-bonds. The disulfide bonds as well as the presence of hydrophobic core are treated as factors responsible for III-order stabilization in proteins. In this protein, the high stability is reached (and ensured) by both factors since the structure of hydrophobic core is almost perfect. Analysis of the role of disulfide bonds in relation to the structure of hydrophobic core was discussed in [43] revealing quite differentiated spectrum from high accordance with the hydrophobic core structure to clear opposite relation where the SS-bond fragments represent highly discordant (in respect to expected

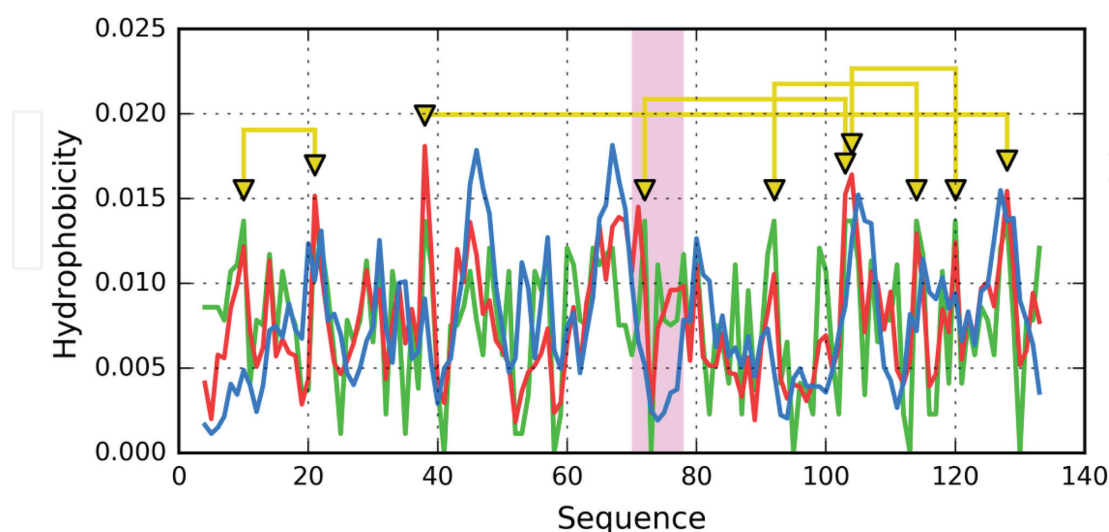


Figure 4. T and O distributions in a type II antifreeze protein (2ZIB). The main discordant section (exposure of hydrophobicity) has been marked on the horizontal axis. Disulfide bonds shown as yellow lines.

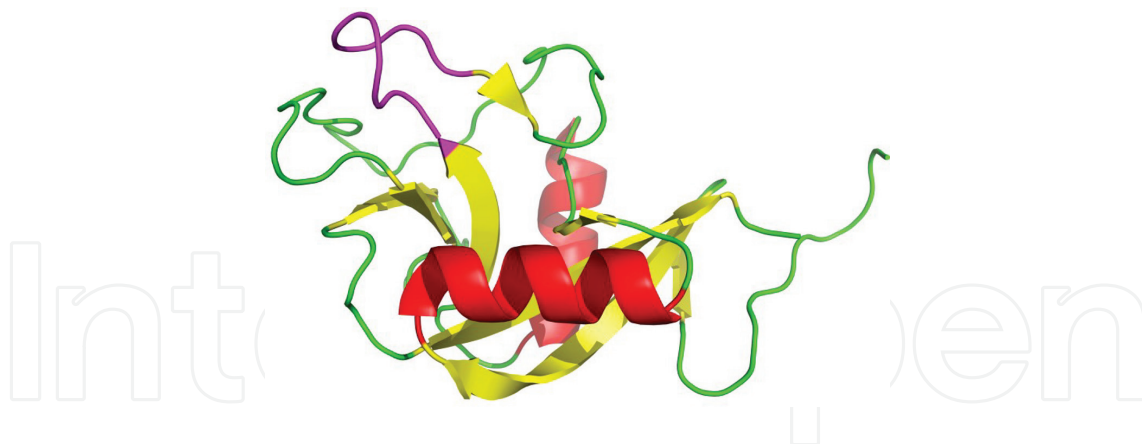


Figure 5. 3D (2ZIB) view with the 70-78 fragment highlighted in pink. This fragment represents excess hydrophobicity on the protein surface. Rest of the molecule represents the status accordant with 3D Gauss distribution of hydrophobicity.

one) formation of hydrophobic core. The presence of so many SS-bonds may additionally support stabilization of the structure as it is expected for antifreeze protein to be resistant to the influence of the surrounding.

3.3. Antifreeze protein which contains a solenoid fragment

5B5H provides an example of an antifreeze protein which contains a solenoid fragment. A general description of this protein can be found in [16]. It is classified as a multidomain protein (even though this is not reflected by the CATH [44, 45] specification stored in PDBsum [46, 47]). In this case, the concept of “multiple domains” appears to relate to the presence of diverse secondary structural motifs. T, O, and H distributions for this protein are visualized in **Figure 6**, revealing the fragments of variable alignment between profiles.

Table 3 presents the characteristics of this protein taking secondary fragments as individual units. The structure, taken as a whole, is regarded as discordant (**Figure 7A**). However some distinguished fragments appear to represent the distribution accordant with idealized distribution.

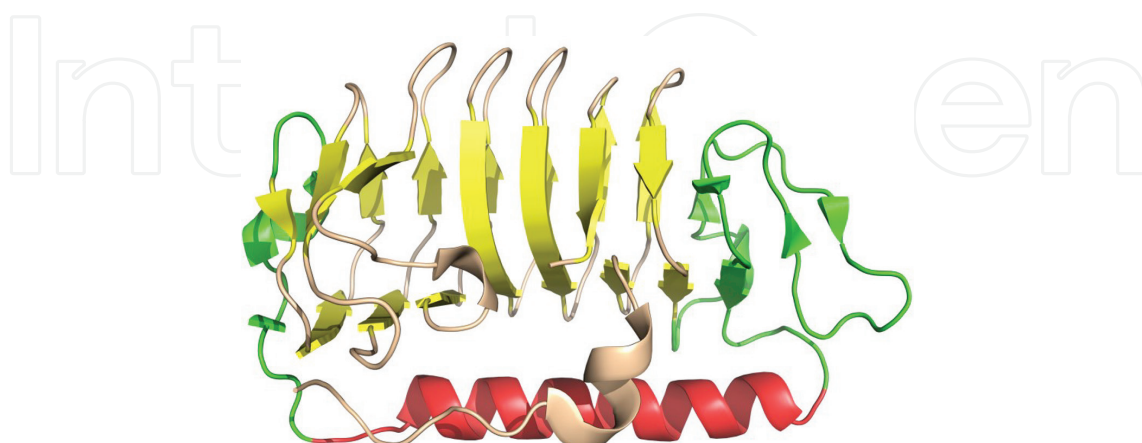


Figure 6. 3D structure of a multidomain antifreeze protein (5B5H). Fragments marked in color are discussed in details. The colors of fragments follow the colors used in **Figure 7**.

5B5H FRAGMENT	RD		Correlation coeff.		
	T-O-R	T-O-H	HvT	TvO	HvO
Entire protein	0.676	0.538	0.386	0.436	0.754
N-stop 37-73	0.649	0.645	0.318	0.502	0.743
C-stop 98-113	0.304	0.093	0.298	0.810	0.421
Solenoid	0.669	0.526	0.386	0.436	0.754
Helix 74-98	0.389	0.431	0.551	0.835	0.688

Table 3. Quantitative description of 5B5H and its selected secondary structural components.

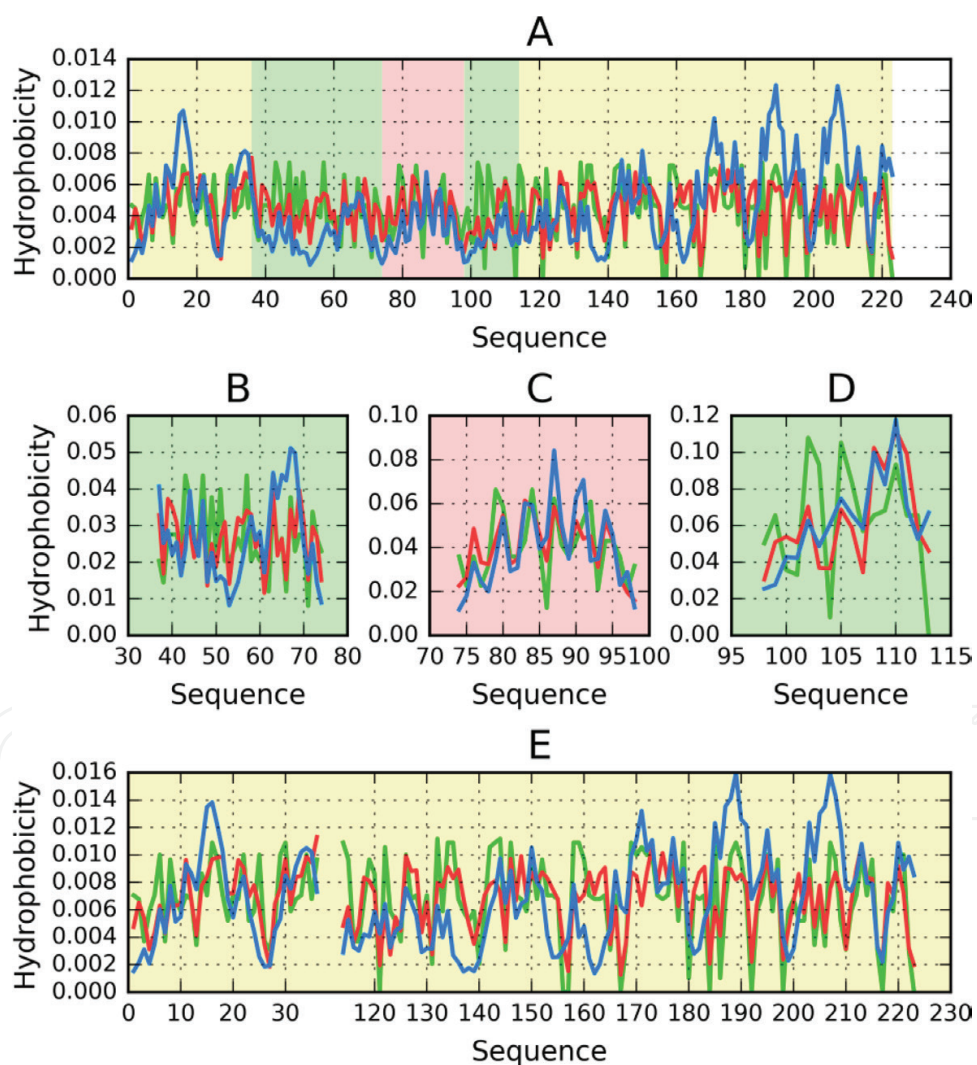


Figure 7. T (blue), O (red) and H (green) distributions for 5B5H. The profiles for colour highlighted fragments are shown individually in B, C and D. A—complete protein, B—N-terminal fragment, C—helix parallel to the solenoid, D—“stop” helix, E—solenoid fragment.

The solenoid (as observed in other examples of proteins) [16] represents the linear propagation of local maxima and minima of hydrophobicity. That is why to prevent the unlimited propagation, the “stop” fragments are necessary. Their status is expected to be accordant with the model. It means that their role is to allow water to penetrate and in consequence prevent uncontrolled grow of fibril.

N-terminal “stop” fragment seems not to play such role as its status is discordant (**Figure 7B**).

Helix—the status of the helix running along the solenoid is accordant with the fuzzy oil drop model, that is, its polar side is exposed to the solvent, while the hydrophobic side remains in contact with the solenoid (**Figures 6 and 7C**). It suggests its role to ensure the solubility of the entire molecule.

“Stop” helix C-terminal, the solenoid, by itself, is susceptible to unrestricted linear propagation, which theoretically may propagate in unlimited form (for example, by complexation of many solenoids). This undesirable effect is prevented by the presence of a short C-terminal helix (**Figures 6 and 7D**) which remains accordant with the theoretical model: polar residues are exposed to the environment, while hydrophobic residues face the solenoid. The helix therefore acts as a “cap”, which prevents elongation of the solenoid. Notably, this is the most accordant fragment within the entire protein (as evidenced by its TvO correlation coefficient)—meaning that its conformation is driven by the tendency to generate a hydrophobic core. Similar “caps” (or “stop” fragments) can be found in many other proteins which include solenoid fragments, and the phenomenon may be exploited in designing drugs which arrest the propagation of amyloid fibrils [48].

Much like an amyloid fibril, the solenoid fragment is characterized by negative correlation coefficients for certain β -structural fragments, which suggests that it actively counteracts the natural tendency for the protein to generate a centralized hydrophobic core.

* Solenoid fragment (**Figures 6 and 7E**; marked in yellow) is the structural core of the protein. In this fragment, the observed distribution of hydrophobicity adopts a sinusoidal pattern with no distinct central peak. High accordance between O and H distribution can be seen. Additionally, the expected hydrophobicity concentration (high blue picks **Figure 7E**) is not present. Recurring fluctuations reflect both the symmetry of the solenoid itself and the arrangement of residues in the chain. Such alternating bands of high and low hydrophobicity are thought to affect the structural properties of the solvent—water molecules, which are attracted to hydrophilic patches but repelled by hydrophobic patches are also likely to adopt a linear “bandlike” structure. In [49], the authors suggest, and the experimentally prove, that water levitates above hydrophobic surfaces. This phenomenon, in turn, increases the mobility of water particles, as proved in [42].

3.4. Amyloid protein—A β structure (1-40)

Amyloids have a significant impact on the surrounding solvent. Here, we present the beta amyloid (1-40). This molecule meets the criteria specified in [17, 18] by exhibiting linear propagation of alternating bands of high and low hydrophobicity, which clearly deviate from the monocentric Gaussian in favor of a different structural pattern. The β -amyloid (1-40) structure [30] will be analyzed as a superfibril, as a protofibril and as well as an individual chain (component of the protofibril).

3.4.1. $A\beta(1-40)$ superfibril

The structure listed in PDB under the ID 2MVX comprises two individual protofibrils arranged symmetrically (C_2 symmetry). Each protofibril resembles a flattened letter C. These protofibrils are connected by their tips, with their “backs” facing outward. **Figure 8** presents the theoretical and observed distributions of hydrophobicity for the superfibril when analyzed as a whole. Clearly, in place of a monocentric peak of hydrophobicity, we are instead dealing with a sinusoidal pattern expressed along the fibril’s axis. This type of distribution is typical for amyloids and results from structural repeatability of the input chain, as well as from the symmetry between both protofibrils. In the T-O-R model, the RD value of the superfibril is 0.590, while in the T-O-H model, it is equal to 0.592, with correlation coefficients of 0.438, 0.673, and 0.727 for HvT, TvO, and HvO, respectively. These values suggest that the superfibril adopts a conformation which does not involve a central hydrophobic core. It moreover indicates that the resulting structure represents a compromise between the tendency to generate a hydrophobic core and the intrinsic properties of individual amino acids comprising the sequence.

The distribution illustrated in **Figure 8** reveals the expected (T) concentration of hydrophobicity in the central part of the fibril. The sinusoidal shape of the intrinsic (H) and observed (O) distribution curves is due to the previously postulated linear propagation of alternating bands of high and low hydrophobicity—a characteristic feature of amyloids [17, 18].

Figure 9 also reveals a repetitive pattern of alternating peaks and troughs, propagating along the chains. It should be noted that this single chart (red) represents several individual chains (shaped like a stack of sheets—on top of and beneath the sheet on which the chart is printed), each of which is characterized by identical arrangement of local maxima and minima. The variability seen in **Figure 9A** is related to the properties of edge chains which—being adjacent to only one other chain rather than two—exhibit slightly lower hydrophobicity than chains which make up the fibril’s interior (**Figure 9B**). It is these interior chains which should be regarded as particularly representative for the amyloid form, owing to their capability for unrestricted propagation (observed both *in vitro* and *in vivo*).

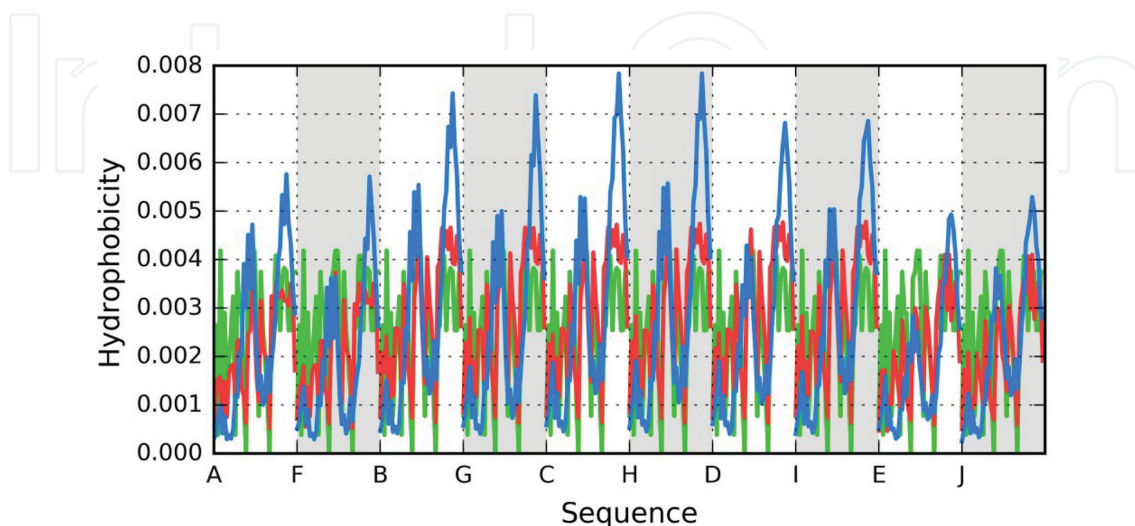


Figure 8. H (green), T (blue) and O (red) distributions for the $A\beta(1-40)$ super-fibril (2MVX). White and gray backgrounds distinguish two proto-fibrils.

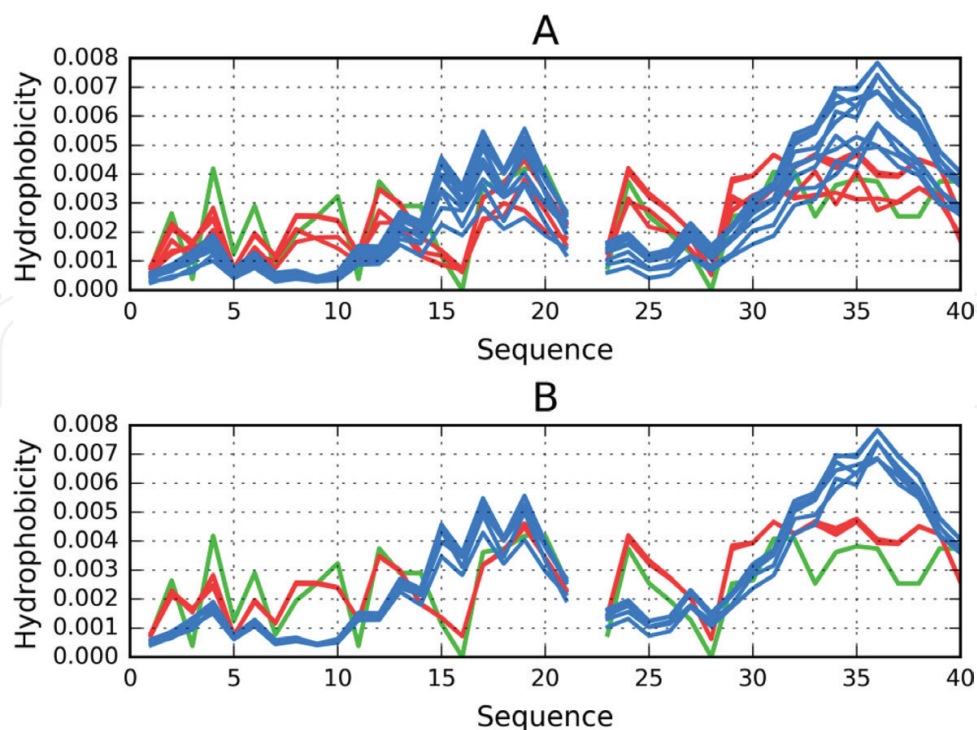


Figure 9. T (blue), H (green) and O (red) distributions for: A—all chains making up the super-fibril B—all chains except edge chains (AEFJ).

Plotting the theoretical 3D Gaussian for the entire complex (superfibril) enables us to assess the status of interface fragments, which include residues in contact with adjacent protofibrils. These residues have been analyzed in accordance with PDBSUM criteria [14]. The resulting RD values for the interface fragments are 0.432 and 0.387 for T-O-R and T-O-H, respectively, with correlation coefficients equal to 0.378, 0.672, and 0.658 for HvT, TvO, and HvO, respectively. These values suggest the status of the interface as accordant with the theoretical distribution of hydrophobicity as given by the fuzzy oil drop model, as long as the complex is analyzed as a whole (note the high values of TvO and HvO coefficients, indicating that the observed distribution is in agreement with both theoretical and the intrinsic distribution).

The above observations enable us to speculate that protofibrils are dominated by the intrinsic hydrophobicity of individual residues, leading to linear propagation of alternating bands of high and low hydrophobicity. In contrast, the complex (consisting of two protofibrils) is shaped by forces related to the presence of the aqueous solvent.

3.4.2. Structure of the $A\beta(1-40)$ protofibril

Analysis of individual protofibrils has been performed on the basis of T, O, and H distributions, with the theoretical distribution (T) plotted for the single protofibril rather than for the entire complex. Each protofibril comprises five chains labeled A, B, C, D, and E. **Figure 10** illustrates the relevant distributions of hydrophobicity.

Again, we observe a repeating sinusoidal pattern instead of the expected central peak. The observed distribution is a result of the highly symmetrical arrangement of chains which form the protofibril and of their sequential identity (**Figure 10** and **Figure 11**).

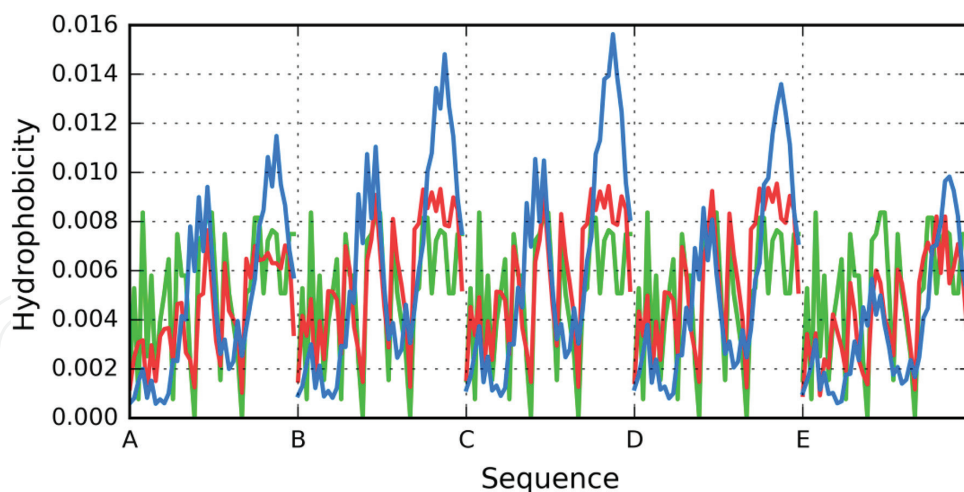


Figure 10. T (blue), O (red) and H (green) distributions for the A β (1-40) proto-fibril (chains ABCDE).

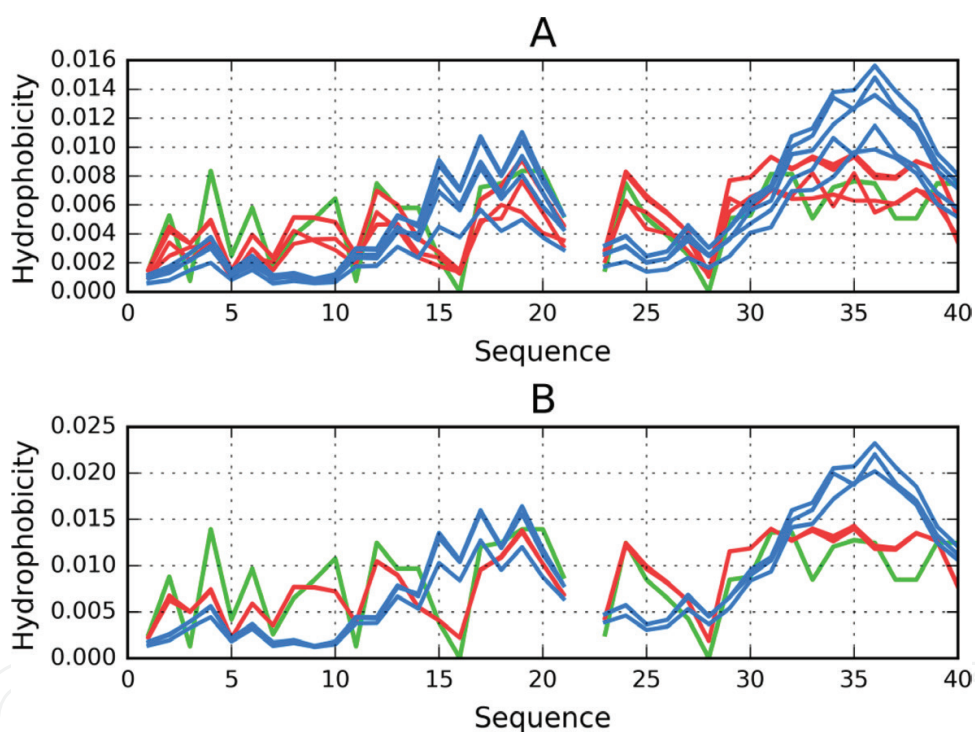


Figure 11. Status of protofibril (Chains ABCDE)—T(blue), O(red), H(green). A—all chains shown, B—central chains (BCD)—the border chains removed to show the almost identical distribution in central chains.

The status of the protofibril is described by the following parameters: RD (T-O-R): 0.639; RD (T-O-H): 0.659. This means that the involvement of intrinsic hydrophobicity in shaping the protofibril's structure is greater than in the case of the superfibril. Correlation coefficients are 0.280, 0.365, and 0.718 for HvT, OvT, and HvO, respectively. This further shows that the conformation of the protofibril is dominated by the intrinsic hydrophobicity of its residues.

3.4.3. Structure of an individual chain present in A β (1-40) protofibril

The status of the C chain (i.e., the central chain in the protofibril) is visualized in **Figure 12**. The chart reveals strong dominance of intrinsic hydrophobicity (**Figure 12A**) with the consequent

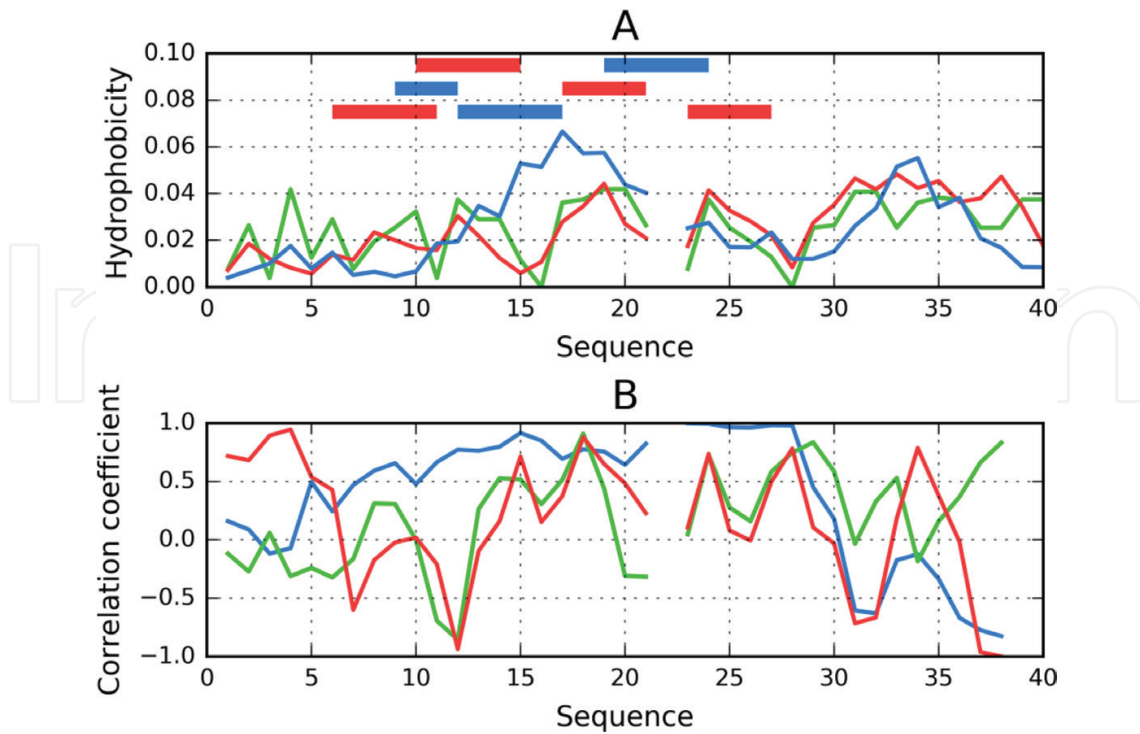


Figure 12. A β (1-40) hydrophobicity profiles (2MVX). A—T(blue), O(red) and H(green) distributions. Horizontal lines correspond to local maxima (red) interspersed with local minima (blue). B—Correlation coefficients calculated for successive 5aa fragments to visualize the status of sequential 5 aa fragments (HvO—blue, TvO—red, HvT—green).

lack of alignment with the theoretical monocentric distribution (T). Comparing correlation coefficients for successive 5 aa fragments singles out the fragments at 9-16 and 22-27 as particularly discordant.

It should be noted that the charts plotted in **Figure 12A** and **B** for the central chain are also representative for all chains forming the protofibril, regardless of their length. The presence of local maxima and minima which are inconsistent with the theoretical (T) distribution applies to all chains. In this particular case, we can observe a local maximum at 7-9 (contrary to T, which predicts a local minimum), a local minimum at 9-11 (in place of the expected increase in hydrophobicity), then another maximum at 10-15, a minimum at 14-17 (where the T distribution predicts a global peak), a minimum at 22, and another local maximum at 22-27. The C-terminal fragment is consistent with the theoretical distribution; however, the calculated RD values and correlation coefficients confirm strong discordance vs. T (**Table 4**).

Figure 13 provides a visualization of the linear propagation of alternating bands of high and low hydrophobicity.

Such linear arrangement of alternating bands can be expected to have an impact upon the properties of the aqueous environment. Experimental research, which focuses on water in contact with hydrophobic surfaces, suggests that under such circumstances, levitation of water particles may occur [49]. This phenomenon provides water particles with greater mobility, which, in turn, disfavors the formation of ice crystals. Since similar conditions are encountered on the surface of amyloids and antifreeze proteins, we may speculate that water does indeed gain increased mobility when in contact with amyloids—perhaps even interfering with the action of proteolytic enzymes [50], which are known not to degrade amyloid

Fragment	RD		Correlation coeff.		
	T-O-R	T-O-H	HvT	TvO	HvO
1-40	0.649	0.686	0.310	0.322	0.779
7-9	0.509	0.459	0.812	0.589	0.795
9-11	0.522	0.808	-0.227	0.135	0.934
10-15	0.776	0.815	-0.330	-0.566	0.855
14-17	0.493	0.269	0.425	0.275	0.913
16-22	0.427	0.359	0.477	0.521	0.947
22-27	0.509	0.460	0.242	0.190	0.987
27-40	0.615	0.545	0.352	0.577	0.719

Fragments listed in boldface exhibit strong amyloid characteristics.

Table 4. Status of the C chain (the central one in protofibril) and its individual fragments—RD values (T-O-R; T-O-H) and correlation coefficients (HvT, TvO, and HvO).

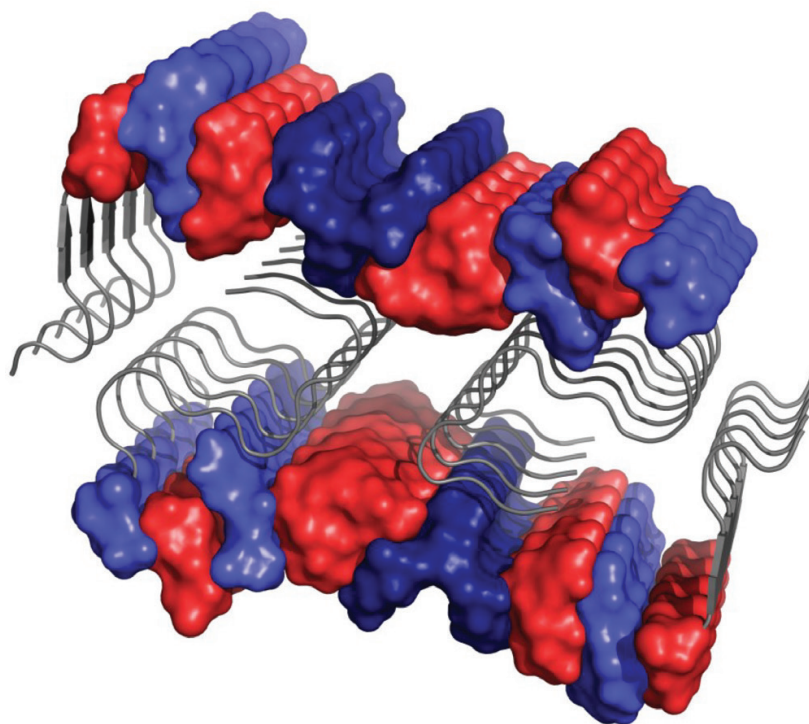


Figure 13. 3D presentation of 2MVX, highlighting local maxima (red) (8-9, 12-13, 17-19, and 23-24) and minima (blue) (10-11, 14-16, 20-21, and 25-26) (dark blue—fragment 14-16 with the minimum which is against the expected maximum—see **Figure 11A**) of hydrophobicity, as observed in A β (1-40). The linear propagation of discordant fragments along the fibril's axis can be readily observed. It is possible to put here the arrows (as shown in **Figure 3**) to visualize the predicted variability in the structural properties of water (with orientation toward hydrophilic surfaces regarded as more likely), showing how the peculiar conditions occurring on the protein's surface disrupt the natural structuralization of the solvent.

fibrils. In effect, the enzyme fails to recognize the “signal” generated by an aberrant protein. Additionally, the amyloid protein is deprived of any fragments of structure accordant with the model as it is observed in antifreeze proteins, which act as native, biologically active proteins which undergo standard degradation procedure.

4. Conclusions

The analysis presented in this chapter, along with numerous other publications which deal with the fuzzy oil drop model, suggests that deviations from the theoretical distribution of hydrophobicity in a protein (i.e., exposure of hydrophobic and/or hydrophilic residues on the surface) are strongly linked with biological activity. This effect clearly disrupts the natural structuralization of the surrounding solvent and forces it to adapt itself to the protein's presence. In light of the presented analysis, the protein may be perceived as a more or less imperfect micelle (whether spherical, flattened, worm-like or cylindrical), devoid of the strong symmetries observed in surfactant micelles. Such imperfections (i.e., deviations from a perfectly symmetrical micelle) enable the protein to perform its intended function by interacting with other molecules (ligands or external proteins); however, such local deviations from optimal water-protein interactions also have an effect on the aqueous solvent itself. The degree to which the protein deviates from the ideal (theoretical) distribution of hydrophobicity is also a measure of the changes induced in its environment; such changes may be regarded as a means of communication and a carrier of information. This observation echoes the underlying assumptions of the so-called iceberg model [32].

The influence of water upon the native form of proteins remains an open issue—particularly in the context of local discordances, which are disadvantageous from the perspective of protein-solvent interactions. It is uncertain whether such discordances are only due to the nature of the residue sequence, which cannot produce a fully ordered micelle, or whether some other factors are at play. On the other hand, it is evident that such local disruptions affect the properties of the solvent (viewed as a continuum). It can also be demonstrated—on the grounds of the fuzzy oil drop model—that local deviations from the theoretical distribution of hydrophobicity are targeted and encoded information concerning the protein's biological activity [51].

Our approach likens the protein to an “intelligent micelle” which imposes a specific local disorder within the aqueous solvent and thereby encodes a description of the required protein-water interaction. A surfactant micelle—being perfectly symmetrical—carries no such information. In a similar vein, antifreeze proteins that are highly consistent with the theoretical distribution of hydrophobicity (such as the type II antifreeze protein [16]) perform their function simply by being present in the solvent and do not need to encode any specific information.

It appears that experimental research focusing on such “imperfect” micelles and on their interaction with the environment may yield clues regarding the function of proteins and, in particular, their specificity. Under these assumptions, the structure of the protein represents a very delicate balance between micelle-like ordering (which provides the protein with solubility) and local deviations, whose purpose is complex. On the one hand, such deviations encode the capacity to perform a specific chemical reaction as a result of inter-molecular contact; on the other hand, they represent signals which manifest themselves by the changes in the solvent as it adapts itself to the presence of the protein.

The solenoid fragment included in certain antifreeze proteins produces more or less parallel bands with very different structural properties in the surrounding medium. Whatever

the ordering in the neighborhood of hydrophobic bands, it definitely does not resemble the structure observed near hydrophilic bands. Experimental studies indicate that water gains increased mobility at the boundary between bands [42, 49]. Such dynamic properties may prevent formation of ice crystals, which otherwise calls for highly uniform conditions in the bulk medium. Nevertheless, the antifreeze protein is not merely a solenoid—it also includes other fragments (with diverse secondary structural characteristics), mediating optimal interaction with the water environment. While similar linear arrangement can be observed in amyloids, they differ from antifreeze proteins in the sense that their ideal periodicity is dependent on the sequential identity of each complexed chain. We may speculate that under such conditions, the aberrant protein issues a signal which cannot be recognized by other proteins—this would explain why enzymes do not interact with the amyloid.

The concept of reorganization of the aqueous solvent may even be approached from a rheological perspective [52].

The mechanisms employed by antifreeze proteins resemble those exploited on a macroscopic scale by humans—for example, inducing mobility (e.g., by stirring, which prevents freezing) or by introducing factors which produce structural changes in the medium, disfavoring the formation of ice (such as salting). The “tasks” performed by ancillary fragments of the antifreeze protein are associated with the specific nature of the environment in which proteins operate—in particular, their role is to ensure solubility. A precipitated antifreeze protein would be useless; hence, the long helix runs parallel to the solenoid and ensures solubility by limiting the “disorder” which the solenoid fragment induces. The list of similarities between macroscopic processes and molecular-scale phenomena exploited by living organisms is long. A more detailed discussion of the subject can be found in [53].

The information encoded by a 3D structure concerns not only the specifics of a molecular process (lowering the energy threshold for enzymatic reactions) but also—or perhaps most importantly—the means by which different molecules may communicate with one another. Substrate recognition is not merely based on a “lock and key” mechanism. The participating molecules must first recognize each other, and this recognition may exploit distortions in the structure of the aqueous solvent. Under this hypothesis, the solvent acts as a carrier of information, which is specific enough to be recognized by the intended recipient. Significant research interest has recently been directed at biological systems in dried-out conditions (such as seeds [54]). When most of the solvent is eliminated from the system, leaving only enough water to preserve the 3D conformation of proteins (as in a dry seed), communication effectively ceases. However, this change is reversible, and communication can be restored simply by adding water—this causes the seed to resume its biological function and germinate.

Acknowledgements

The authors wish to thank Piotr Nowakowski and Anna Śmietańska for editorial assistance. This research has been supported by Jagiellonian University Collegium Medicum grant no. K/ZDS/006363.

Author details

Mateusz Banach¹, Leszek Konieczny² and Irena Roterman^{1*}

*Address all correspondence to: irena.roterman-konieczna@uj.edu.pl

1 Department of Bioinformatics and Telemedicine, Jagiellonian University – Medical College, Kraków, Poland

2 Chair of Medical Biochemistry, Jagiellonian University – Medical College, Krakow, Poland

References

- [1] Anfinsen CB. The formation and stabilization of protein structure. *The Biochemical Journal*. 1972;**128**(4):737-749
- [2] Anfinsen CB. Principles that govern the folding of protein chains. *Science*. 1973;**181**(4096):223-230
- [3] Dobson CM. Protein folding and misfolding. *Nature*. 2003;**426**(6968):884-890
- [4] Hartl FU. Molecular chaperones in cellular protein folding. *Nature*. 1996;**381**(6583):571-579
- [5] Dill KA, Ozkan SB, Shell MS, Weikl TR. The protein folding problem. *Annual Review of Biophysics*. 2008;**37**:289-316
- [6] Muñoz V, Cerminara M. When fast is better: Protein folding fundamentals and mechanisms from ultrafast approaches. *Biochemical Journal*. 2016;**473**(17):2545-2559
- [7] <https://www.ebi.ac.uk/casp1/Casp1.html>
- [8] Berendsen HJ, Van Gunsteren WF, Zwinderman HR, Geurtsen RG. Simulations of proteins in water. *Annals of the New York Academy of Sciences*. 1986;**482**:269-286
- [9] Van Gunsteren WF, Berendsen HJ. Molecular dynamics: Perspective for complex systems. *Biochemical Society Transactions*. 1982;**10**(5):301-305
- [10] Van Der Spoel D, Lindahl E, Hess B, Groenhof G, Mark AE, Berendsen HJ. GROMACS: Fast, flexible, and free. *Journal of Computational Chemistry*. 2005;**26**(16):1701-1718
- [11] Piwowar M, Banach M, Konieczny L, Roterman I. Hydrophobic core formation in protein complex of cathepsin. *Journal of Biomolecular Structure & Dynamics*. 2014;**32**(7):1023-1032
- [12] Banach M, Konieczny L, Roterman I. The fuzzy oil drop model, based on hydrophobicity density distribution, generalizes the influence of water environment on protein structure and function. *Journal of Theoretical Biology*. 2014;**359**:6-17

- [13] Bryliński M, Prymula K, Jurkowski W, Kochańczyk M, Stawowczyk E, Konieczny L, Roterman I. Prediction of functional sites based on the fuzzy oil drop model. *PLoS Computational Biology*. 2007;**3**(5):e94
- [14] Dygut J, Kalinowska B, Banach M, Piwowar M, Konieczny L, Roterman I. Structural interface forms and their involvement in stabilization of multidomain proteins or protein complexes. *International Journal of Molecular Sciences*. 2016;**17**(10):E1741
- [15] Brylinski M, Kochanczyk M, Broniatowska E, Roterman I. Localization of ligand binding site in proteins identified in silico. *Journal of Molecular Modeling*. 2007;**13**(6-7):665-675
- [16] Banach M, Konieczny L, Roterman I. Why do antifreeze proteins require a solenoid? *Biochimie*. 2018;**144**:74-84
- [17] Roterman I, Banach M, Konieczny L. Application of the fuzzy oil drop model describes amyloid as a ribbonlike micelle. *Entropy*. 2017;**19**(4):167
- [18] Roterman I, Banach M, Kalinowska B, Konieczny L. Influence of the aqueous environment on protein structure—A plausible hypothesis concerning the mechanism of amyloidogenesis. *Entropy*. 2016;**18**(10):351
- [19] Kelley EG, Murphy RP, Seppala JE, Smart TP, Hann SD, Sullivan MO, Epps TH. III Size evolution of highly amphiphilic macromolecular solution assemblies via a distinct bimodal pathway. *Nature Communications*. 2014;**5**:3599
- [20] Nisticò R, Scalarone D, Magnacca G. Sol-gel chemistry, templating and spin-coating deposition: A combined approach to control in a simple way the porosity of inorganic thin films/coatings. *Microporous and Mesoporous Materials*. 2017;**248**:18-29
- [21] Huang J, Hang S, Feng Y, Li J, Yan H, He F, Wang G, Liu Y, Wang L. Rheological properties and application of wormlike micelles formed by sodium oleate/benzyltrimethyl ammonium bromide. *Colloids and Surfaces A: Physicochemical and Engineering Aspects*. 2016;**500**:222-229
- [22] Kumar S, Awang MB, Abbas G, Kalwar SA. Wormlike micellar solution: Alternate of polymeric mobility control agent for chemical EOR. *Journal of Applied Sciences*. 2014;**14**:1023-1029
- [23] Sarvi MN, Stevens GW, Gee ML, O'Connor AJ. The co-micelle/emulsion templating route to tailor nano-engineered hierarchically porous microspheres. *Microporous and Mesoporous Materials*. 2012;**149**(1):101-105
- [24] Liu N, He Q, Wang Y, Bu W. Stepwise self-assembly of a block copolymer–platinum(II) complex hybrid in solvents of variable quality: From worm-like micelles to free-standing sheets to vesicle-like nanostructures. *Soft Matter*. 2017;**13**:4791-4798
- [25] Patel V, Ray D, Singh K, Abezgauz L, Marangoni G, Aswal VK, Bahadur P. 1-Hexanol triggered structural characterization of the worm-like micelle to vesicle transitions in cetyltrimethylammonium tosylate solutions. *RSC Advances*. 2015;**5**:87758-87768

- [26] Konieczny L, Brylinski M, Roterman I. Gauss-function-based model of hydrophobicity density in proteins. *In Silico Biology*. 2006;**6**(1-2):15-22
- [27] Liepinsh E, Otting G, Harding MM, Ward LG, Mackay JP, Haymet AD. Solution structure of a hydrophobic analogue of the winter flounder antifreeze protein. *European Journal of Biochemistry*. 2002;**269**(4):1259-1266
- [28] Nishimiya Y, Kondo H, Takamichi M, Sugimoto H, Suzuki M, Miura A, Tsuda S. Crystal structure and mutational analysis of Ca²⁺-independent type II antifreeze protein from longsnout poacher, *Brachyopsis rostratus*. *Journal of Molecular Biology*. 2008;**382**(3):734-746
- [29] Cheng J, Hanada Y, Miura A, Tsuda S, Kondo H. Hydrophobic ice-binding sites confer hyperactivity of an antifreeze protein from a snow mold fungus. *The Biochemical Journal*. 2016;**473**(21):4011-4026
- [30] Schütz AK, Vagt T, Huber M, Ovchinnikova OY, Cadalbert R, Wall J, Güntert P, Böckmann A, Glockshuber R, Meier BH. Atomic-resolution three-dimensional structure of amyloid β fibrils bearing the Osaka mutation. *Angewandte Chemie (International Ed. in English)*. 2015;**54**(1):331-335
- [31] Kalinowska B, Banach M, Konieczny L, Roterman I. Application of divergence entropy to characterize the structure of the hydrophobic core in DNA interacting proteins. *Entropy*. 2015;**17**(3):1477-1507
- [32] Kauzmann W. Some factors in the interpretation of protein denaturation. *Advances in Protein Chemistry*. 1959;**14**:1-63
- [33] Kyte J, Doolittle RF. A simple method for displaying the hydropathic character of a protein. *Journal of Molecular Biology*. 1982;**157**(1):105-132
- [34] Levitt M. A simplified representation of protein conformations for rapid simulation of protein folding. *Journal of Molecular Biology*. 1976;**104**(1):59-107
- [35] Kullback S, Leibler RA. On information and sufficiency. *Annals of Mathematical Statistics*. 1951;**22**(1):79-86
- [36] Kalinowska B, Banach M, Wiśniowski Z, Konieczny L, Roterman I. Is the hydrophobic core a universal structural element in proteins? *Journal of Molecular Modeling*. 2017;**23**(7):205
- [37] Ben-Naim A. Myths and verities in protein folding theories: From Frank and Evans iceberg-conjecture to explanation of the hydrophobic effect. *The Journal of Chemical Physics*. 2013;**139**(16):165105
- [38] Bar Dolev M, Braslavsky I, Davies PL. Ice-binding proteins and their function. *Annual Review of Biochemistry*. 2016;**85**:515-542
- [39] Walters KR Jr, Serianni AS, Sformo T, Barnes BM, Duman JG. A nonprotein thermal hysteresis-producing xylomannan antifreeze in the freeze-tolerant Alaskan beetle *Upis ceramboides*. *Proceedings of the National Academy of Sciences of the United States of America*. 2009;**106**(48):20210-20215

- [40] Miskowiec A, Buck ZN, Hansen FY, Kaiser H, Taub H, Tyagi M, Diallo SO, Mamontov E, Herwig KW. On the structure and dynamics of water associated with single-supported zwitterionic and anionic membranes. *Chemical Physics*. 2017;**146**(12):125102
- [41] Fletcher GL, Hew CL, Davies PL. Antifreeze proteins of teleost fishes. *Annual Review of Physiology*. 2001;**63**:359-390
- [42] Modig K, Qvist J, Marshall CB, Davies PL, Halle B. High water mobility on the ice-binding surface of a hyperactive antifreeze protein. *Physical Chemistry Chemical Physics*. 2010;**12**(35):10189-10197
- [43] Banach M, Kalinowska B, Konieczny L, Roterman I. Role of disulfide bonds in stabilizing the conformation of selected enzymes—An approach based on divergence entropy applied to the structure of hydrophobic core in proteins. *Entropy*. 2016;**18**(3):67
- [44] CATH. <http://www.cathdb.info/>
- [45] Dawson NL, Lewis TE, Das S, Lees JG, Lee D, Ashford P, Orengo CA, Sillitoe I. CATH: An expanded resource to predict protein function through structure and sequence. *Nucleic Acids Research*. 2017;**45**(D1):D289-D295
- [46] de Beer TAP, Berka K, Thornton JM, Laskowski RA. PDBsum additions. *Nucleic Acids Research*. 2014;**42**:D292-D296
- [47] <http://www.ebi.ac.uk/>
- [48] Roterman I, Banach M, Konieczny L. Propagation of fibrillar structural forms in proteins stopped by naturally occurring short polypeptide chain fragments. *Pharmaceuticals*. 2017;**10**(4):89
- [49] Schutzius TM, Jung S, Maitra T, Graeber G, Köhme M, Poulidakos D. Spontaneous droplet trampolining on rigid superhydrophobic surfaces. *Nature*. 2015;**527**(7576):82-85
- [50] Saido T, Leissring MA. Proteolytic degradation of amyloid β -protein. *Cold Spring Harbor Perspectives in Medicine*. 2012;**2**(6):a006379
- [51] Banach M, Konieczny L, Roterman I. Secondary and supersecondary structure of proteins in light of the structure of hydrophobic cores. In: Alexander K, editor. *Methods in Molecular Biology Protein Supersecondary Structures*. Vol. 2. Springer. (in press)
- [52] Georgiev MT, Danov KD, Kralchevsky PA, Gurkov TD, Krusteva DP, Arnaudov LN, Stoyanov SD, Pelan EG. Rheology of particle/water/oil three-phase dispersions: Electrostatic vs. capillary bridge forces. *Journal of Colloid and Interface Science*. 2018; **513**:515-526
- [53] Konieczny L, Roterman I, Spólnik P. *Systems Biology – Functional Strategies of Living Organisms*. New York, Heidelberg, Dordrecht, London: Springer; 2013
- [54] Gordon ME, Payne PI. In vitro translation of the long-lived messenger ribonucleic acid of dry seeds. *Planta*. 1976;**130**:269-273

